WILEY Applied Organometallic Chemistry

Crown ether functionalized magnetic hydroxyapatite as eco-friendly microvessel inorganic-organic hybrid nanocatalyst in nucleophilic substitution reactions: an approach to benzyl thiocyanate, cyanide, azide and acetate derivatives

Maedeh Azaroon[1] 🔘 | Ali Reza Kiasat[1,2]

[1] Chemistry Department, College of Science, Shahid Chamran University of Ahvaz, Ahvaz, Iran

[2] Petroleum Geology and Geochemistry Research Centre, (PGGRC), Shahid Chamran University of Ahvaz, Ahvaz, Iran

Correspondence
Maedeh Azaroon, Chemistry Department, College of Science, Shahid Chamran University of Ahvaz, Ahvaz, Iran.
Email: m-azaroon@phdstu.scu.ac.ir

In this paper, high catalytic activity of $4',4''$-diformyl dibenzo-18-crown-6 anchored onto the functionalized magnetite hydroxyapatite (γ-Fe$_2$O$_3$@HAp–Crown) as a new, versatile and magnetically recoverable catalyst, was prepared. It evaluated as phase-transfer catalyst and molecular host system for nucleophilic substitution reactions of benzyl halides with thiocyanate, cyanide, azide and acetate anions in water. No evidence for the formation of by-products was observed and the products obtained in pure form without further purification. The nanocomposite was easily removed from solution via application of a magnetic field, allowing straightforward recovery and reuse. The synthesized nanocomposite was characterized by several techniques such as FT-IR, TGA-DTG, EDX, XRD, BET, FE-SEM, TEM and VSM.

KEYWORDS
$4',4''$-diformyl dibenzo-18-crown-6, Fe$_2$O$_3$@HAp-crown, nucleophilic substitution reaction, phase-transfer catalyst

1 | INTRODUCTION

The unique structure and properties of macrocyclic crown ethers (CEs) have made them a popular choice for a wide range of investigations and applications over the past few decades. They play major roles in many disciplines such as supramolecular chemistry, analytical chemistry, catalysis and phase-transfer catalysis.[1–4] CEs serve as simple receptor models and are well-suited as hosts because of their conformational flexibility, hydrophilic cavity and the presence of multiple binding sites that endow them with a special ability to accommodate many organic compounds by inclusion complexation because they can be linked both non-covalently and covalently.[5–7] In addition, the rather high selectivity of the many interesting chemical reactions in the presence of crown ethers was achieved due to their excellent ability as a selective neutral host for charged metal ions in its narrow cavity and activation of anion species in many circumstances.[8–11]

Nowadays, magnetic nanoparticles have attracted considerable interest due to their easy separation and also their remarkable physical and chemical properties.[12–15] To avoid the aggregation of nanoparticles and to improve their chemical stability, the surface of the nanoparticles has been coated with different materials, such as silica, MCM-41, polymer and hydroxyapatite.[16–23] Among them hydroxyapatite, a mineral form of calcium apatite, which is shown by Ca$_{10}$(PO$_4$)$_6$(OH)$_2$ has several unique properties such as lower cost of production, availability and environment friendly nature which can make hydroxyapatite-encapsulated magnetic nanocrystallites an excellent support for the preparation of heterogeneous catalysts in organic chemistry.[24–38]

Crown ethers performing as excellent phase-transfer catalyst in asymmetric reactions have been reported in several papers, with high enantioselectivities and yields observed applying these compounds; in this work, hydroxyapatite coated uniform γ-Fe_2O_3 core-shell particles were synthesized and crown ether immobilized on an insoluble support presents can lead to the formation of novel nanocomposites, which combines and enhances the characteristics of the components, such as the electronic, thermal, and catalytic properties and molecular recognition of the macrocyclic hosts. With this goal in mind and in continuation of ongoing research into the employment of grafted diformyl dibenzo-18-crown-6 ether as a stationary micro-vessel and heterogeneous catalyst in organic transformations,herein, we report our results on the preparation and characterization of a novel organic–inorganic magnetic nanocomposite, γ-Fe_2O_3@HAp-Crown, and explored its application in the nucleophilic substitution reactions as a proficient, harmless to the environment, recyclable and magnetic powerful solid catalyst with good stability.

2 | EXPERIMENTAL

2.1 | General remarks

Iron (II) chloride tetrahydrate (99%), iron (III) chloride hexahydrate (98%), 3,4-Dihydroxy benzaldehyde, benzyl halides, and other chemicals were purchased from Fluka and Merck companies and used without further purification. NMR spectra were recorded in $CDCl_3$ on a Bruker Advance DPX 400 MHz instrument spectrometer using TMS as internal standard The purity determination of the products and reaction monitoring were accomplished by TLC on silica gel. Products were characterized by comparison of their physical and spectral data (^{1}H NMR, ^{13}C NMR and FT-IR spectra) with those reported in the literature.

The surface area and pore size distribution of the support was measured by the nitrogen adsorption–desorption method (Belsorp mini II). FT-IR (Fourier transform infrared) spectra were recorded on a Perkin-Elmer (IL74XB3GV5) spectrometer. X-ray diffraction (XRD) patterns of catalyst were taken on Philips X-ray diffraction model Research (PANalytical Company). The field emission scanning electron micrograph (FE-SEM) was obtained by FE-SEM instrumentation (MIRA3TESCAN-XMU). Energy-Dispersive X-ray spectroscopy (EDX) analysis was obtained by MIRA3TESCAN-XMU instrument. Transmission electron microscope (TEM) images were obtained using Zeiss – EM10C –80 kV instrument. The TGA curve was recorded on a PC Luxx 409 at heating rates of 10 °C min^{-1}. The magnetic properties were investigated with a vibrating magnetometer (Meghnatis Daghigh Kavir Co., Kashan, Iran).

2.2 | Preparation of mesoporous magnetite–hydroxyapatite nanoparticles anchored dibenzo-18-crown-6 ether, γ-Fe_2O_3@HAp –crown

2.2.1 | Preparation of aminopropyl conjugated mesoporous magnetite–hydroxyapatite

First, the mixture of $FeCl_2.4H_2O$ (1.85 mmol) and $FeCl_3.6H_2O$ (3.7 mmol) were dissolved in deionized water (30 ml) under Ar atmosphere at room temperature and the resulting solution was added to a 25 wt % NH_4OH solution (10 ml) with vigorous mechanical stirring. A black precipitate of Fe_3O_4 was produced instantly. In order to obtain small and uniform Fe_3O_4 particles, the drop rate of NH_4OH was controlled precisely by a constant dropper and the drop rate was 1 ml min^{-1}. After 15 min, 100 ml of $Ca(NO_3)_2.4H_2O$ (33.7 mmol, 0.5 M) and $(NH_4)_2HPO_4$ (20 mmol, 3.0 M) solutions adjusted to pH 11 were added drop-wise to the obtained precipitate over 30 min with mechanical stirring. The resulting milky solution was heated to 90 °C. After 2 h, the mixture was cooled to room temperature and aged overnight. The dark brown precipitate formed was filtered, washed repeatedly with deionized water until the water was neutral, and then air-dried under vacuum at room temperature. The synthesized sample was calcinated at 300 °C for 3 h, giving a reddish-brown powder. Then for the linkage of aminopropyl unit to the surface of support, 1 g of the obtained γ-Fe_2O_3 coated HAp, γ-Fe_2O_3@HAP, was dispersed in anhydrous toluene (100 ml), with ultrasonication for 15 min and 3-aminopropyl trimthoxysilane (10 mmol) was added. The mixture was heated under reflux conditions for 24 h under Argon protection. The suspended substance was collected by a magnet and rinsed thoroughly with toluene, and dried under vacuum to give pure 3-aminopropyl-modified magnetite–hydroxyapatite, γ-Fe_2O_3@HAP-NH_2.

2.2.2 | Synthesis of 4′,4″-diformyl dibenzo-18-crown-6 ether

Diethylene glycol ditosylate, DEDT, was firstly synthesized and used as precursor for the synthesis of benzo crown ether according to Pederson's method with suitable adaptation[39,40]; Briefly for the preparation of DEDT[41]; diethylene glycol (14.86 g, 140 mmol) was dissolved in THF (80 ml). Meanwhile, an aqueous solution of sodium hydroxide (16 g, 400 mmol) in water (80 ml) was

prepared. Two solutions were mixed and cooled on ice bath with magnetic stirring. To the above mixture was added drop wise tosyl chloride (48.6 g, 260 mmol) in THF (80 ml) over 2 h with continuous stirring and cooling of mixture below 5 °C. The solution was stirred at 0–5 °C for additional 2 h, after this, the mixture was poured into ice-water (250 ml). The DEDT product was filtered, washed with distilled water, dried and recrystallized twice from methanol to give a pure product in 80% isolated yield.

Then for the synthesis of 4′,4″-diformyl dibenzo-18-crown-6 ether, DFBCE, a mixture of 3,4-dihydroxy benzaldehyde (8.28 g, 60 mmol), and sodium hydroxide pellets (2.44 g, 60 mmol) in 1-butanol (40 ml) was refluxed under argon for 30 min to ensure complete dissolution of sodium hydroxide. A solution of DEDT (12.36 g, 30 mmol) in 1-butanol (20 ml) was added slowly over 1 h, and the mixture was refluxed for 1 h. The temperature was lowered to 90 °C and sodium hydroxide pellets (2.44 g) was added. Refluxing was continued for 30 min and DEDT (12.36 g, 30 mmol) in 1-butanol (20 ml) was added slowly over 1 h. Refluxing was continued for 16 h. Concentrated hydrochloric acid (1 ml) was slowly added, and then 1/3 of solvent was rapidly removed by distillation. The distillation was continued but the volume in the flask was kept constant by the steady addition of water until the vapor temperature reached 100 °C. The mixture was filtered, washed with 200 mL of water, and sucked dry. The DFBCE product was dispersed in 200 ml of acetone, stirred for 30 min, filtered, washed with 50 ml of acetone, and dried in an oven at 100 °C.

2.2.3 | Preparation of magnetite–hydroxyapatite anchored dibenzo-18-crown-6 ether

DFBCE (0.624 g, 1.5 mmol) was dissolved in $CHCl_3$ (50 ml) and refluxed to complete dissolving of crown ether. γ-Fe_2O_3@HAP-NH_2 (1 g) was added to the mixture and refluxed for 24 h. The precipitate, γ-Fe_2O_3@HAp –Crown, was washed and redispersed with deionized water and ethanol several times. The particles were finally collected using a magnet and dried at 50–60 °C for 12 h.

2.2.4 | General procedure for the nucleophilic substitution reaction catalyzed by Fe_2O_3@HAp-crown nanocomposite in water

In a typical experiment, to a mixture of the benzyl halide (1.0 mmol) and NaY (Y: SCN, N_3, OAc, CN) (2 mmol) in water (5 ml), Fe_2O_3@HAp-Crown (0.08 g) was added and heated under stirring condition at 80 °C for the time specified in Table 3. After complete consumption of starting material as judged by TLC (n-hexane–ethyl acetate), the catalyst was separated on the sidewall of the reaction vessel using an external magnet, the aqueous phase was separated by decantation and extracted with diethyl ether (3 × 5 ml). After extraction, the organic layer was dried with $CaCl_2$ and evaporated in vacuum to give corresponding product in 75–95% yields. The residual catalyst in the reaction vessel was washed and dried and then subjected to the next run directly.

3 | RESULTS AND DISCUSSION

Dibenzo-18-crown-6-ether supported on HAp-encapsulated-γ-Fe_2O_3, Fe_2O_3@HAp-Crown, was synthesized according to the procedure shown in Scheme 1 and 2. Maghemite-nanoparticles are commonly synthesized by coprecipitation of ferrous and ferric ions in a basic aqueous solution followed by thermal treatment. Because of the sensitivity of the γ-Fe_2O_3, its surface was first coated with hydroxyapatite. For grafting dibenzo-18-crown-6-ether moieties onto the surface of the γ-Fe_2O_3@HAp, the aminopropyl groups were preliminarily bonded onto the surface of magnetic hydroxyapatite. After that, the dibenzo-18-crown-6-ether was covalently grafted onto the surface of the core/shell magnetic nanostructure by simple condensation reaction (Scheme 1 and 2).

To characterize the nanocomposite, and to confirm the immobilization of the active components on the pore surface of magnetite–hydroxyapatite, Fourier transform infrared spectroscopy (FT-IR) was utilized. Figure 1a-d shows the FT-IR spectra of the Fe_2O_3@HAp (a), Fe_2O_3@HA-NH_2 (b), Fe_2O_3@HAp-Crown (c) and DFBCE (d), respectively. According to the spectra, characteristic
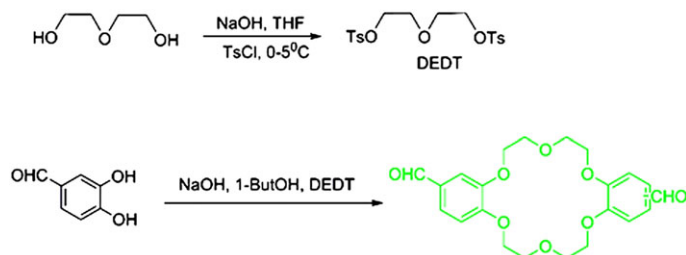
SCHEME 1 Synthetic procedure of 4′,4″-diformyl dibenzo-18-crown-6
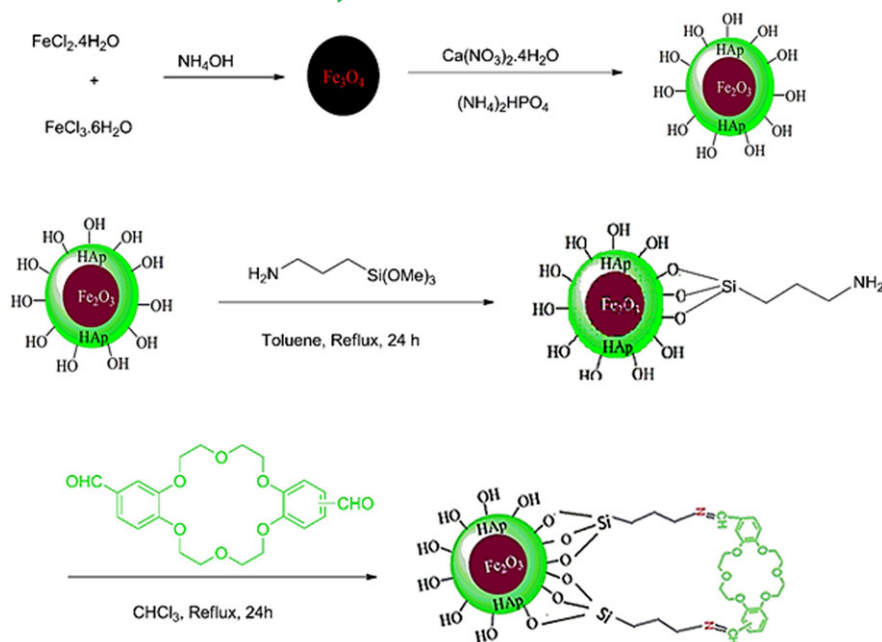
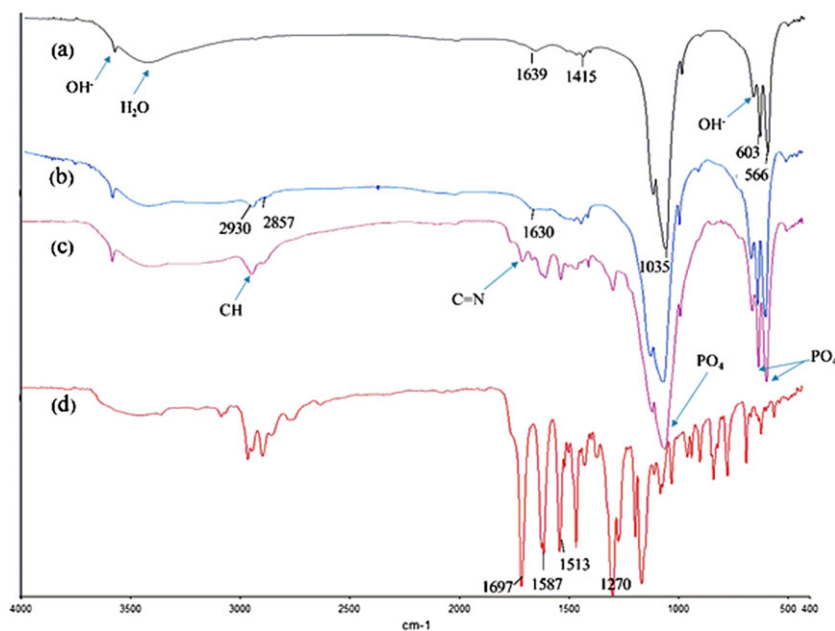**SCHEME 2** Synthetic route for preparation of γ-Fe₂O₃@HAp-Cown

FIGURE 1 The FT-IR spectra of (a) γ-Fe₂O₃@HAp, (b) γ-Fe₂O₃@HAp-NH₂, (c) γ-Fe₂O₃@HAp-crown and (d) DFBCE

absorption bands due to the bending vibration mode of -O–P–O surface phosphate groups in the Hydroxyapatite were observed at 566 and 603 cm^{-1} which overlap with Fe–O bonds stretching, the adsorption band at 1035 cm^{-1} can be attributed to the stretching of the P–O bond (Figure 1a-c). The peaks at 3571 and 632 cm^{-1} are due to OH^- ions. The broad Bands in 3420 cm^{-1} and around 1639 cm^{-1} arise from water, the 1415 cm^{-1} peak are from CO_3^{2-} ions. For Fe₂O₃@HAp-NH₂ (Figure 1b), peaks at 2930 cm^{-1} and 1631 cm^{-1} were assigned to stretching vibration of C-H bonds of the propyl-amine groups and -NH stretching vibrations. The spectrum of DFBCE (Figure 1d) displayed characteristic peaks at 1270 cm^{-1}, 1513 cm^{-1} and 1587 cm^{-1} were also observed in spectrum of γ-

Fe₂O₃@HAp-Crown with little shift (Figure 1c). The peak at 1688 cm^{-1} was assigned to imin band in γ-Fe₂O₃@HAp-Crown, show DFBCE was covalently grafted onto the surface of Fe₂O₃@HAp-NH₂ (Figure 1d). The result provides direct evidence that the conjugation occurs.

Thermo-gravimetric analysis- Derivative thermo-gravimetric Analysis (TGA-DTG) is a useful method for the determination of the presence or absence of residual components of the catalysts. It is based on the observation of the mass loss of individual components. The stability of γ-Fe₂O₃@HAp-Crown was examined by TGA-DTG were shown in Figure 2.

The curves show that three distinct steps of weight loss in the combined TGA-DTG curves. The first weight loss of
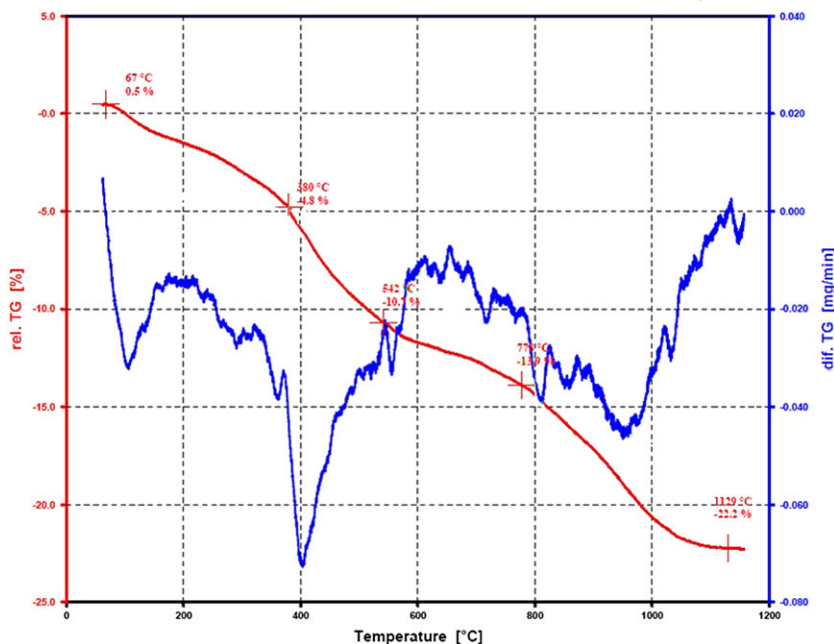
FIGURE 2 A typical TGA curve of γ-Fe$_2$O$_3$@HAp-crown catalyst

0.5% below 200 °C which might be due to the loss of the adsorbed water as well as dehydration of the surface OH groups. The second weight loss step of about 30% in the region of 380–780 °C come from the decomposition of organic substances in Fe$_2$O$_3$@HAp-Crown composite. After that, there was a weight loss from 800 °C to 1000 °C due to the decomposition of calcium carbonate to calcium oxide which verified the presence of hydroxyapatite.

γ-Fe$_2$O$_3$@HAp and γ-Fe$_2$O$_3$@HAp-Crown nanocomposite were subject to further structural characterization with Energy Dispersive X-ray spectroscopy (EDX) spectrum (Figure 3). As clearly observed, in addition of Ca, P, O and Fe elements, which are present in the magnetite–hydroxyapatite (Figure 3a), presence of C, N and Si are indicated on the γ-Fe$_2$O$_3$@HAp-Crown (Figure 3b). The results proved that DFBCE were successfully grafted onto the surface of γ-Fe$_2$O$_3$@HAp.

Typical X-ray diffraction (XRD) patterns of the γ-Fe$_2$O$_3$@HAp-Crown catalyst are shown Figure 4 The peaks at 2θ = 35.7°, 43.6°, 53.3°, 57.1° and 63.1° are attributed to γ-Fe$_2$O$_3$ (marked), in agreement with the standard reflection peaks (JCPOS card 25–1402), Hydroxyapatite also shows typical diffraction peaks, (marked O), at 2θ = 25.7°, 31.8°, 32.9°, 34.1°, 39.8°, 46.8°, and 49.4° (PDF-2-no. [084–1998] (ICDD)).[27] The functionalization process on the surface of γ-Fe$_2$O$_3$@HAp to produce γ-Fe$_2$O$_3$@HAp-Crown nanocomposite have no obvious effect on the formation of well crystallized solid with sharp and strong peaks. This result indicates that supporting of DFBCE on γ-Fe$_2$O$_3$@HAp does not change the support structure.

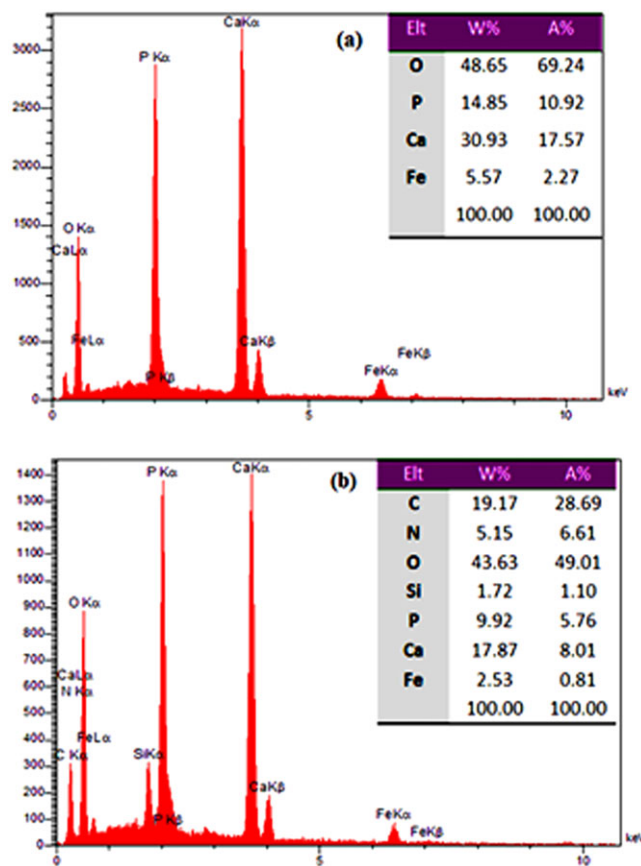Figure 5 represent the low temperature nitrogen adsorption–desorption isotherms and pore size

Elt	W%	A%
O	48.65	69.24
P	14.85	10.92
Ca	30.93	17.57
Fe	5.57	2.27
	100.00	100.00

Elt	W%	A%
C	19.17	28.69
N	5.15	6.61
O	43.63	49.01
Si	1.72	1.10
P	9.92	5.76
Ca	17.87	8.01
Fe	2.53	0.81
	100.00	100.00

FIGURE 3 EDX spectrum of γ-Fe$_2$O$_3$@HAp(a) and γ-Fe$_2$O$_3$@HAp-crown(b)

distributions of γ-Fe$_2$O$_3$@HAp and γ-Fe$_2$O$_3$@HAp-Crown samples which exhibit a type IV curve with a hysteresis loop. Type IV isotherms correspond to a mesoporous material. According to the report in Table 1 about Brunauer–Emmett–Teller (BET) surface area, pore
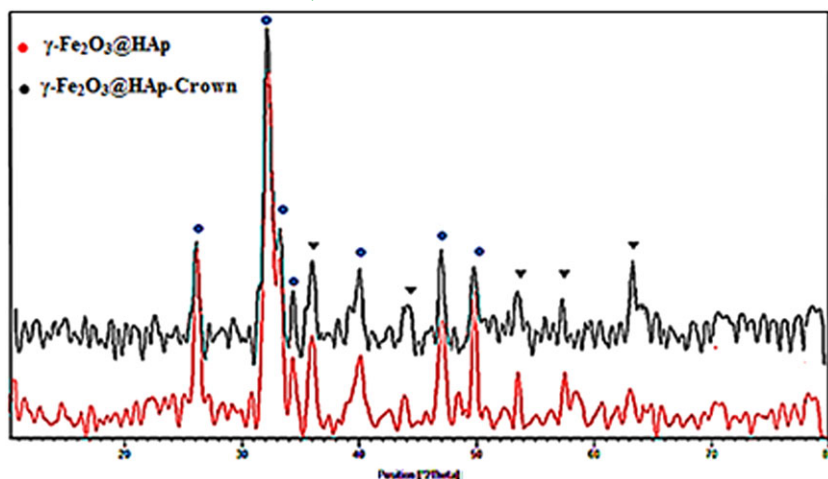
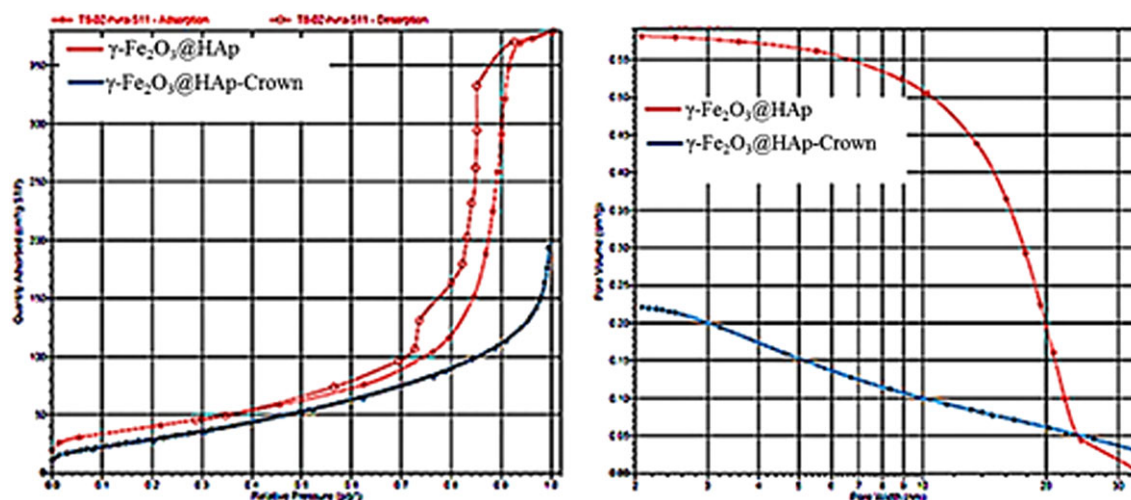**FIGURE 4** XRD patterns of γ-Fe₂O₃@HAp and γ-Fe₂O₃@HAp-crown

FIGURE 5 Nitrogen adsorption/desorption isotherms (left) and pore size distributions curves (right) of γ-Fe₂O₃@HAp and γ-Fe₂O₃@HAp-crown

TABLE 1 Comparison of the textural properties of γ-Fe₂O₃@HAp and γ-Fe₂O₃@HAp-crown

Samples	BET surface area [m²/g]	Pore volume [cm³/g]	Pore size [nm]
γ-Fe₂O₃@HAp	143.97	0.57	15.98
γ-Fe₂O₃@HAp-crown	113.53	0.20	7.22

volume and pore size of Fe_2O_3@HAp (BET: 143.97 m²/g, pore volume: 0.57 cm³/g and pore size: 15.98 nm), decrease in these values after loading crown ethers on Fe_2O_3@HAp is due to this fact that the crown ethers unites were deposited inside the cavities and dispersed on the surface of magnetite–hydroxyapatite.

The morphology and size details were investigated by field emission scanning electron microscopy (FE-SEM) measurement. The FE-SEM images of the γ-Fe₂O₃@HAp and γ-Fe₂O₃@HAp-Crown are presented in Figure 6, clearly shown that the particles have nano size range and their morphology has a round shape. As shown in Figure 6, grafting DFBCE onto the hydroxyapatite shell did not lead to the significant change in the structure and

morphology of nanoparticles, indicating that the magnetic core remained intact during the immobilization and functionalization process on the surface of nanocomposite.

The transmission electron microscopy (TEM) images of the as-prepared Fe_2O_3@HAp-Crown (Figure 7) was clearly shown that the γ-Fe₂O₃@HAp-Crown has a spherical-shaped morphology with slight aggregation. The images indicate that $γ-Fe_2O_3$ (dark spots) was encapsulated by Hap, and particles exhibit a size distribution of 25–30 nm, similar to the sizes obtained from the FE-SEM measurements.

Magnetic properties of γ-Fe₂O₃@HAp, γ-Fe₂O₃@HAp-Crown and Fe_3O_4 were investigated using a vibrating sample magnetometer (VSM) with a field of −10000 Oe
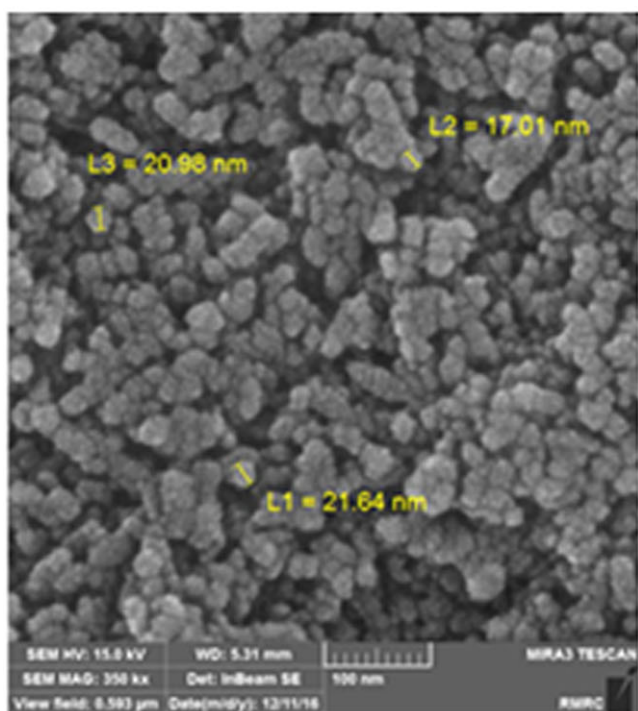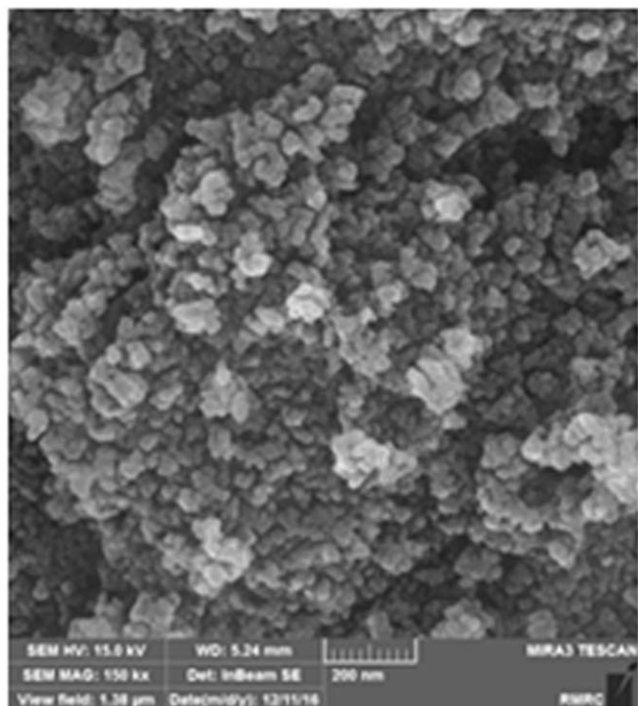
FIGURE 7 TEM image of γ-Fe_2O_3@HAp-crown

FIGURE 6 FE-SEM images of γ-Fe_2O_3@HAp (a), γ-Fe_2O_3@HAp-crown (b)

to 10000 Oe at room temperature. As shown in Figure 8, the M(H) hysteresis loop for the three samples was completely reversible, which indicated their superparamagnetic characteristics. The catalysts γ-Fe_2O_3@HAp and γ-Fe_2O_3@HAp-Crown demonstrated saturation magnetization values of 8.13 emu. g^{-1} and 5.56 emu. g^{-1}, respectively, while the Fe_3O_4 nanoparticle had the value of 54.94 emu. g^{-1}. The reason may be
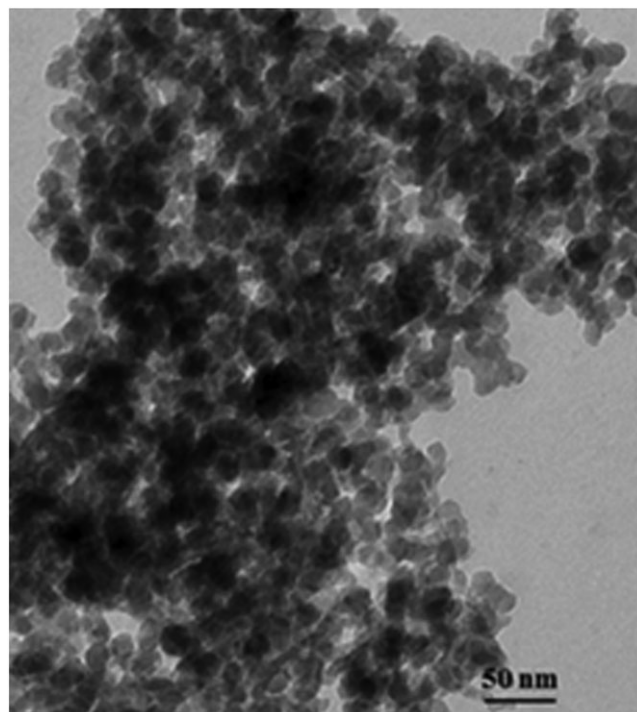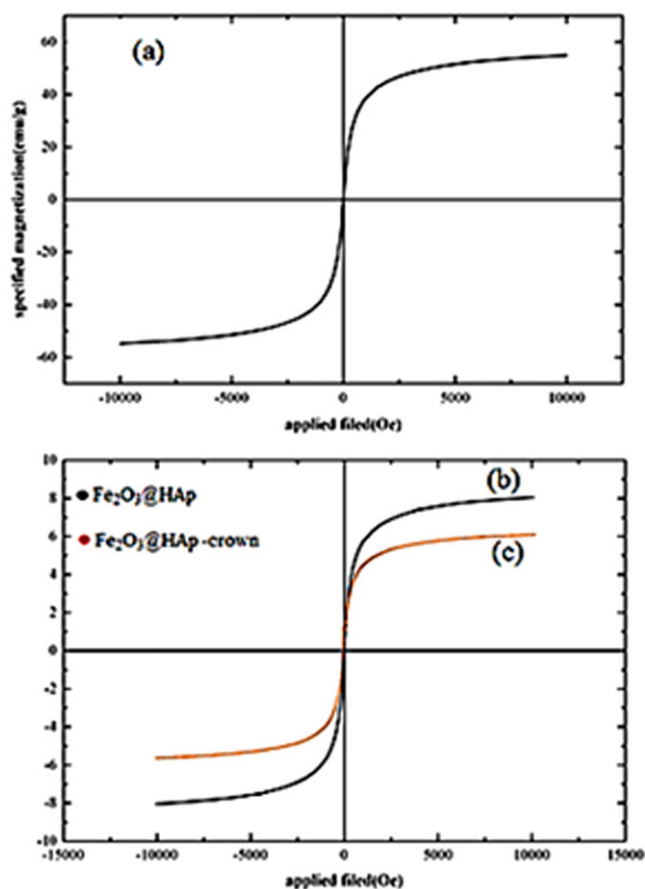
FIGURE 8 Hysteresis loops of Fe_3O_4 (a), γ-Fe_2O_3@HAp (b) and γ-Fe_2O_3@HAp-crown (c)

attributed to the grafting of DFBCE over γ-Fe₂O₃@HAp. However, the lower value of Figure 8b and Figure 8c is still enough to ensure the readily recovery of the catalysts from reaction mixture using external magnetic force.

In order to investigate the possible catalytic properties of the γ-Fe₂O₃@HAp-Crown nanocatalyst in the nucleophilic substitution reaction, the reaction of benzyl halides with thiocyanate anion in water was investigated. Initially, the mixture of benzyl bromide and NaSCN in water was chosen as model reaction to determine whether the use of phase transfer catalyst was efficient and to investigate the optimized reaction conditions (Table 2).

After several set of tests, it was found that the use of 2 equiv. of SCN per benzyl bromide in the presence of the γ-

Fe₂O₃@HAp-Crown (0.08 g) in water under thermal conditions (80 °C), is the best conditions and after stirring for 5 min, the corresponding thiocyanohydrine was obtained in high isolated yield. The collected data for the nucleophilic substitution of thiocyanate anion with various benzyl halides under optimized reaction conditions were shown in Table 3.
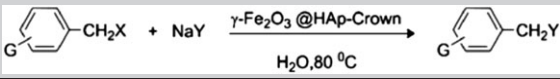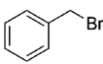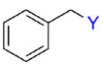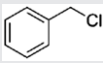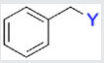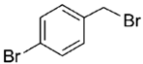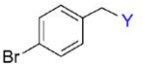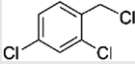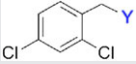
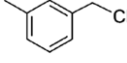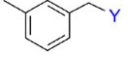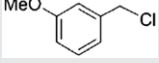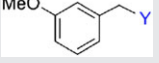This catalyst acted very efficiently and, in all cases, a clean reaction was observed. It is noteworthy that no evidence for the formation of by-products such as alcohols or isothiocyanates was observed and the products were obtained in pure form without further purification. ^{13}C resonance of the −SCN and −NCS groups at ~111 and ~145 ppm, respectively, are very characteristic for thiocyanate and isothiocyanate functionalities.[42] The structures of all of the benzyl thiocyanate and thiocyanate products were determined from their analytical and spectral (IR, ^{1}H and ^{13}C NMR) data and by direct comparison with authentic samples.

^{1}HNMR spectra of the crude products clearly showed the formation of thiocyanate and no evidence for the hydrolysis of benzyl halides to the alcohols was observed, which proved that the reactions proceeded cleanly. On the

TABLE 2 Optimization of the amount of the γ-Fe₂O₃@HAp-crown nanocomposite in the proposed reaction

Entry	Catalyst (g)	Time (min)	Yield (%)
1	-	360	Trace
2	0.05	30	60
4	0.08	5	95
5	0.1	5	95

TABLE 3 Nucleophilic substitution reaction of benzyl halides with different anions in water catalyzed by γ-Fe₂O₃@HAp-crown

Entry	Benzyl halide	Product	Nucleophile (Y)	Time (min)	Yield (%)[a]
1			SCN	5	92
			N₃	10	90
			CN	30	88
			OAc	55	80
2			SCN	5	87
			N₃	15	85
			CN	30	80
			OAc	50	76
3			SCN	80	85
			N₃	90	85
			CN	85	82
			OAc	120	73
4			SCN	45	78
			N₃	60	75
			CN	80	72
			OAc	130	68
5			SCN	15	80
			N₃	20	82
			CN	30	78
			OAc	50	70
6			SCN	40	82
			N₃	50	85
			CN	40	80
			OAc	90	78

[a]All the reactions are carried out under refluxed using 1 mmol of benzyl halide, 2 mmol of different anions, 5 mL of H₂O, 0.08 g of γ-Fe₂O₃@HAp-Crown.

other hand, in the absence of γ-Fe$_2$O$_3$@HAp-Crown, the reaction was sluggish and even after prolonged reaction time, a considerable amount of starting material remained. It is due to this fact that the cavity size of dibenzo-18-crown-6 conforming to the Na$^+$ size, therefore the nucleophilicity of SCN$^-$ anion was improved and so the reaction time reduced (Scheme 3).

With these promising results in hand and establishing the advantages of γ-Fe$_2$O$_3$@HAp-Crown as nanomagnetic phase-transfer catalyst and molecular host system, we focused our attention on another nucleophilic substitution reaction. The conversion of various benzyl halides with electron-withdrawing and electron-donating groups to the corresponding benzyl thiocyanates, cyanides, azides and acetates were also investigated and the results were shown in Table 3, which indicate that the desired products were formed in high yields and no side products were observed.

The most ideal synthetic methodology could be defined as a system wherein 100% atom economy as preserved, the catalyst is recycled, and excess of reagent remains throughout in the medium and does not lose activity for several runs. As shown in Scheme 4, after completion of the reaction, the product was extracted by diethyl ether and so the remained mixture containing 1 mmol of NaSCN and catalyst was reused for another run by adding 1 mmol of NaSCN and benzyl bromide (1 mmol).

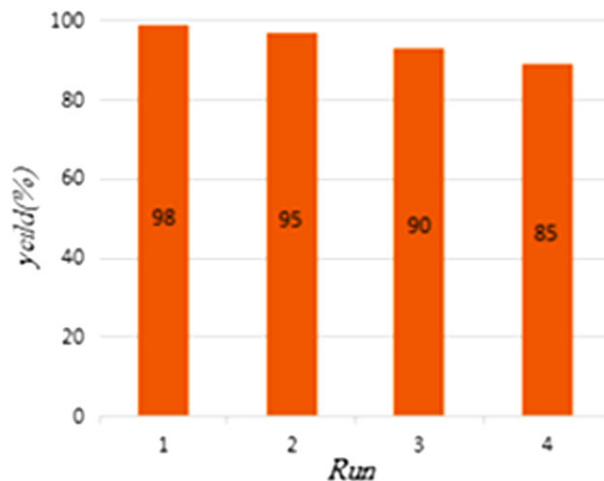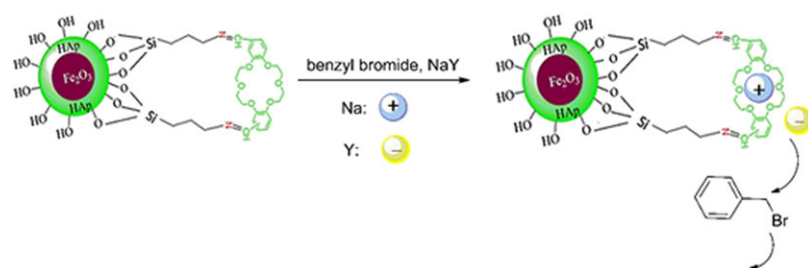The reusability of catalysts is one of the most important benefits of heterogeneous catalytic systems
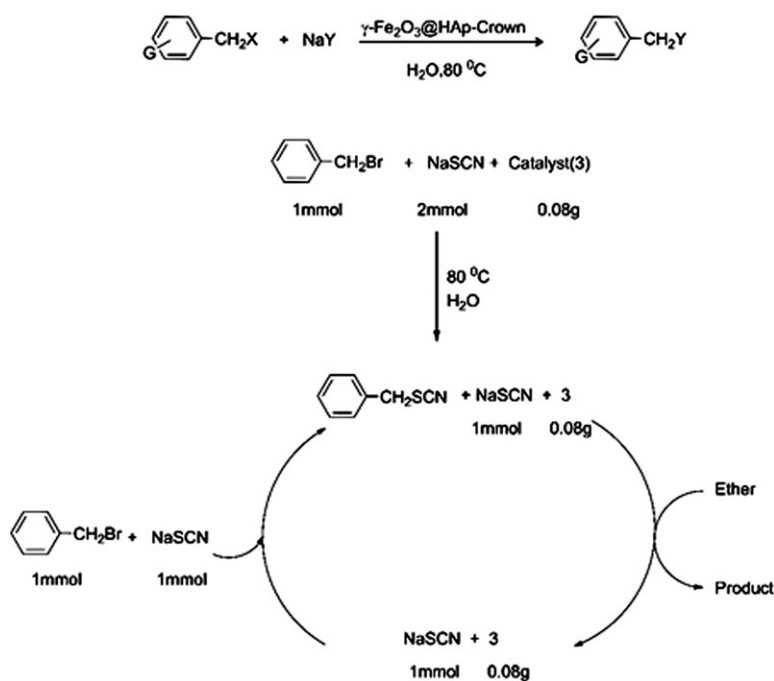
FIGURE 9 Recyclability of catalyst

SCHEME 3 Operation of catalyst in presence of nucleophile salt

SCHEME 4 Facile nucleophilic substitution reaction of benzyl bromide in the atom economical method

TABLE 4 A comparisons of the results of the present system with the some recently reported procedures

Entry	Substrate/ nucleophile	Catalyst and conditions	Time (h)	Yield (%)	Ref.
1	Benzyl bromide/N_3^-	Tetramethylammonium bromide pillared clays/petroleum ether water/100 °C	6	84	[43]
2	Benzyl bromide/N_3^-	Surfactant pillared clay materials and sonochemistry/hexane–water/5 °C	2.5	87	[44]
3	Benzyl bromide/SCN^-	Tetramethylammonium bromide/water/40 °C	1	80	[45]
4	Benzyl chloride/CN^-	Poly [N-(2-aminoethyl) acrylamido] trimethyl ammonium chloride/water/ 100 °C	6.5	88	[46]
5	Benzyl chloride/CN^-	$Ph_3P. Pd(OAc)_2/K_4[Fe(CN)_6]$, Na_2CO_3/140 °C	10	87	[11]
6	Benzyl bromide/SCN^-	n-Bu_4NF-TMSNCS/THF/r.t.	1	98	[4]
7	Benzyl bromide/SCN^-	MNPs-β CD/water/90 °C	0.25	94	[17]
8	Benzylbromide/SCN^-	$Fe_3O_4@SiO_2$/DABCO/100 °C	1	91	[47]
9	Benzyl bromide/SCN^-	β-CDPU-MNPs/water/100 °C	0.08	89	[42]
10	Benzyl bromide/SCN^-	γ-Fe_2O_3@HAp-crown/80 °C	0.08	90	This work

from economic, and environmentally point of view. The recyclability of nanocatalyst was investigated for the nucleophilic substitution reaction between benzyl bromide with thiocyanate anion by carrying out four consecutive cycles using the same reaction conditions. After each run, the catalyst was recovered without filtration since the γ-Fe_2O_3@HAp-Crown was rapidly concentrated as soon as an external magnet was set close to the sidewall of the reaction vessel, then washed with Et_2O (5 ml) and n-hexane (5 ml). The solid catalyst dried under vacuum after each cycle, and then reused for the next reaction (Figure 9).

To demonstrate the superiority of γ-Fe_2O_3@HAp-Crown over the reported catalysts, the reaction of Benzyl bromide and nucleophile was considered as a representative example (Table 4). While in all of these cases, comparative yields of the desired product were obtained following the γ-Fe_2O_3@HAp-Crown catalyzed procedure. These results clearly demonstrate that the nanocomposite is an equally or more efficient catalyst for this reaction.

4 | CONCLUSION

In the present work, the diformyl dibenzo-18-crown-6 ether was successfully grafted on magnetite–hydroxyapatite nanoparticles and its efficiency as solid–liquid phase-transfer catalyst for nucleophilic substitution reactions of benzyl halides in water was also investigated. With the host effects of DFBCE and superparamagnetism of iron oxide, γ-Fe_2O_3@HAp-Crown is expected to have higher potential applications in substitution reactions of benzyl halides. In conclusion, we have developed the easy way to operate, short reaction times, simplicity in operation, high catalytic activity, safe and cost-effective method for the preparation of benzyl thiocyanates, azides, cyanides and acetates in water by nucleophilic substitution reactions.

ORCID

Maedeh Azaroon http://orcid.org/0000-0002-6867-3418

REFERENCES

[1] P. L. Sóti, L. Telkes, Z. Rapi, A. Tóth, T. Vigh, Z. K. Nagy, P. Bakó, G. Marosi, *J. Inorg. Organomet. Polym. Mater.* **2014**, *24*, 713.

[2] A. Mishra, N. Mishra, V. K. Tiwari, *J. Carbohydr. Chem.* **2016**, *35*, 238.

[3] W. Bin Yi, J. J. Ma, L. Q. Jiang, C. Cai, W. Zhang, *J. Fluorine Chem.* **2014**, *157*, 84.

[4] D. Landini, F. Montanari, F. M. Pirisi, *J. Chem. Soc., Chem. Commun.* **1974**, *879*.

[5] B. Gao, S. Wang, Z. Zhang, *J. Inclusion Phenom. Macrocyclic Chem.* **2010**, *68*, 475.

[6] G. H. Rounaghi, M. H. Zavar, R. M. Z. Kakhki, *Russ. J. Coord. Chem.* **2008**, *34*, 167.

[7] W. Taleb Bendiab, F. Hamza Reguig, S. Hamad, B. Martínez-Haya, A. M. Krallafa, *J. Inclusion Phenom. Macrocyclic Chem.* **2016**, *85*, 83.

[8] M. J. Pugia, A. Czech, B. P. Czech, R. A. Bartsch, *J. Org. Chem.* **1986**, *51*, 2945.

[9] S. F. Lee, X. M. Zhu, Y. X. J. Wang, S. H. Xuan, Q. You, W. H. Chan, C. H. Wong, F. Wang, J. C. Yu, C. H. K. Cheng, K. C. F. Leung, *ACS Appl. Mater. Interfaces* **2013**, *5*, 1566.

[10] W. C. Guida, D. J. Mathre, *J. Org. Chem.* **1980**, *45*, 3172.

[11] P. E. Stott, J. S. Bradshaw, W. W. Parish, *J. Am. Chem. Soc.* **1980**, *102*, 4810.

[12] L. H. Reddy, J. L. Arias, J. Nicolas, P. Couvreur, *Chem. Rev.* **2012**, *112*, 5818.

[13] D. Ramimoghadam, S. Bagheri, S. B. Abd Hamid, *Colloids Surf., B* **2014**, *133*, 388.

[14] R. Mrówczyński, A. Nan, J. Liebscher, *RSC Adv.* **2014**, *4*, 5927.

[15] D. Saberi, M. Sheykhan, K. Niknam, A. Heydari, *Catal. Sci. Technol.* **2013**, *3*, 2025.

[16] A. R. Kiasat, S. Nazari, *J. Inclusion Phenom. Macrocyclic Chem.* **2013**, *76*, 363.

[17] J. Davarpanah, A. R. Kiasat, *Catal. Commun.* **2013**, *42*, 98.

[18] G. D. Venkatasubbu, S. Ramasamy, G. S. Avadhani, V. Ramakrishnan, J. Kumar, *Powder Technol.* **2013**, *235*, 437.

[19] J. Liu, S. Z. Qiao, Q. H. Hu, G. Q. Lu, *Small* **2011**, *7*, 425.

[20] A. Ying, H. Hou, S. Liu, G. Chen, J. Yang, S. Xu, *ACS Sustain. Chem. Eng.* **2016**, *4*, 625.

[21] M. J. Nasab, A. R. Kiasat, *RSC Adv.* **2016**, *6*, 41871.

[22] M. B. Gawande, A. Goswami, T. Asefa, H. Guo, A. V. Biradar, D.-L. Peng, R. Zboril, R. S. Varma, *Chem. Soc. Rev.* **2015**, *44*, 7540.

[23] D. Azarifar, M. Ghaemi, *Appl. Organomet. Chem.* **2017**, https://doi.org/10.1002/aoc.3834.

[24] S. Igder, A. R. Kiasat, M. R. Shushizadeh, *Res. Chem. Intermed.* **2015**, *41*, 7227.

[25] Z. Zarei, B. Akhlaghinia, *RSC Adv.* **2016**, *6*, 106473.

[26] A. Mouradzadegun, L. Ma'mani, M. Mahdavi, Z. Rashid, A. Foroumadi, S. Dianat, *RSC Adv.* **2015**, *4*, 1166.

[27] Z. Zhang, J. Zhen, B. Liu, K. Lv, K. Deng, *Green Chem.* **2015**, *17*, 1308.

[28] Y. D. Kwon, D. H. Yang, D. W. Lee, *J. Biomed. Nanotechnol.* **2015**, *11*, 1007.

[29] A. Michelot, S. Sarda, C. Audin, E. Deydier, E. Manoury, R. Poli, C. Rey, *J. Mater. Sci.* **2015**, *50*, 5746.

[30] C. S. Goonasekera, K. S. Jack, J. J. Cooper-White, L. Grøndahl, *J. Mater. Chem. B* **2013**, *1*, 5842.

[31] Z. Zhang, Z. Yuan, D. Tang, Y. Ren, K. Lv, B. Liu, *ChemSusChem* **2014**, *7*, 3496.

[32] Y. Zhang, Z. Li, W. Sun, C. Xia, *Catal. Commun.* **2008**, *10*, 237.

[33] J. A. Ramos Guivar, E. A. Sanches, F. Bruns, E. Sadrollahi, M. A. Morales, E. O. López, F. J. Litterst, *Appl. Surf. Sci.* **2016**, *389*, 721.

[34] H. Liu, F. Chen, P. Xi, B. Chen, L. Huang, J. Cheng, C. Shao, J. Wang, D. Bai, Z. Zeng, *J. Phys. Chem. C* **2011**, *115*, 18538.

[35] N. H. A. Camargo, S. A. de Lima, E. Gemelli, *Am. J. Biomed. Eng.* **2012**, *2*, 41.

[36] M. Sarvestani, R. Azadi, *Appl. Organomet. Chem.* **2017**, https://doi.org/10.1002/aoc.3906.

[37] A. Shaabani, H. Afaridoun, S. Shaabani, *Appl. Organomet. Chem.* **2016**, *30*, 772.

[38] L. Fu, W. Deng, L. Liu, Y. Peng, *Appl. Organomet. Chem.* **2017**, https://doi.org/10.1002/aoc.3853.

[39] C. J. Pedersen, *J. Am. Chem. Soc.* **1967**, *89*, 7017.

[40] S. Yousefi, A. R. Kiasat, *RSC Adv.* **2015**, *5*, 92387.

[41] M. Ough, Y. Inoue, Y. Liu, S. Nagamune, S. Nakamur, K. Wada, T. Hakushi, *Bull. Chem. Soc. Jpn.* **1990**, *63*, 1260.

[42] A. R. Kiasat, S. Nazari, *J. Mol. Catal. A: Chem.* **2012**, *365*, 80.

[43] R. S. Varma, K. P. Naicker, *Tetrahedron Lett.* **1998**, *39*, 2915.

[44] R. S. Varma, K. P. Naicker, D. Kumar, *J. Mol. Catal. A: Chem.* **1999**, *149*, 153.

[45] A. R. Kiasat, R. Badri, S. Sayyahi, *Chinese Chem. Lett.* **2008**, *19*, 1301.

[46] B. Tamami, S. Ghasemi, *J. Iran. Chem. Soc.* **2008**, *5*, S26.

[47] A. R. Kiasat, J. Davarpanah, *J. Mol. Catal. A: Chem.* **2013**, *373*, 46.

SUPPORTING INFORMATION

Additional Supporting Information may be found online in the supporting information tab for this article.